

proximately described by the respective parameters: $L_A = 2.5 L_\odot$, $T_A = 3900$ K, $A_V = 0.9$ (same value for both components), $L_B = 0.25 L_\odot$, $T_B = 3800$ K. There appears to be an infrared excess over a blackbody photosphere on the primary component of SR9, indicating the presence of a probable accretion disk. This example illustrates the advantage of a high angular resolution 3–5 μm imaging detector.

6. Conclusion

We have used ADONIS + SHARP / COMIC to determine the SED of close PMS binaries in the full 1–5 μm range. This new instrument available at the 3.6-m telescope at ESO is very well suited for such scientific programmes. We have used this result to determine the physical characteristics of both components of these close binaries. To take full advantage of the 3–5 μm window on ADONIS + COMIC would require beam-switching

observations, but this is not possible with the current ADONIS setting. We therefore recommend to calibrate the close background emission by measuring it regularly (less than every hour or so) on a sky position empty of sources close to the object position. This appears particularly important if one wishes to observe extended sources like galaxies. The SED fitting procedure provides an approximate value for the visual absorption and the effective temperature. The access of the COMIC instrument to the 3–5 μm window will allow us to detect the presence of accretion disks around close binary components and study the relation of these disks with separation. A more precise determination of the spectral type of our binary targets will await the availability of the *GraF* adaptive optics infrared spectrometer currently under tests at ESO.

Acknowledgements. The adaptive optics observations would not have

been possible without the constant help and support of the ESO ADONIS team, and we are happy to thank here the ESO ADONIS team for its great help and enthusiasm during the run. Hervé Geoffroy acknowledges one year of ESO studentship during which this study has been performed.

References

- Devillard, N., 1997, *The Messenger*, **87**, 19.
 Ghez et al. 1993, *AJ*, **106**, 200.
 Herbig, G.H., and Bell, K.R., 1988, *Third Catalog of Emission-Line Stars of the Orion Population*, Lick Observatory Bulletin series.
 Lacombe et al., 1997, submitted.
 Leinert et al. 1993, *A&A*, **278**, 12.
 Marco et al., 1997, submitted.
 Monin et al., 1997, in *Poster Proceedings of IAU Symp. No. 182*, eds. Malbet & Castets, (1997), p. 230.
 Reipurth & Zinnecker, 1993. *A&A*. **278**, 81.

E-mail address:

Jean-Louis.Monin.@obs.ujf-grenoble.fr

An ESO 3.6-m/Adaptive Optics Search for Young Brown Dwarfs and Giant Planets

W. BRANDNER¹, J.M. ALCALÁ², S. FRINK³, and M. KUNKEL⁴

¹University of Illinois at Urbana-Champaign, USA

²Osservatorio Astronomico di Capodimonte, Napoli, Italy

³Astronomisches Rechen-Institut Heidelberg, Germany

⁴Max-Planck-Institut für Astronomie, Heidelberg, Germany

1. Extrasolar Planets and the Brown Dwarf Gliese 229 B

Only two years ago, the century-old paradigm that other planetary systems would be similar to our own solar system started to change. The discovery of extrasolar giant planets and brown dwarfs by monitoring radial velocities of nearby stars revealed that giant planets are not necessarily 5 to 30 AU away from their sun but may orbit at much smaller ($\ll 1$ AU) separations (Mayor & Queloz, 1995, Marcy & Butler, 1996).

While radial velocity surveys are most successful for discovering close companions, direct imaging allows one to probe systems with larger separations for which radial velocity methods are not sensitive. Indeed, Gl 229B, the first brown dwarf to be identified unambiguously, has a separation of 45 AU from the central star. It was discovered with an adaptive optics coronagraph at the Palomar 1.5-m telescope (Nakajima et al., 1995, Oppenheimer et al., 1995). Direct imaging of resolved objects also allows one to study their spectral features in detail.

As inferred by Allard & Hauschildt (1995) from computations of model at-

mospheres, the energy distribution of late-type dwarfs (and thus of young brown dwarfs and giant planets) is very peculiar. The molecular opacities that globally define the continuum cause the spectral energy distribution to peak around 1.1 μm for solar metallicities, almost independently of the effective temperature.

In Figure 1 we show on top a low-resolution spectrum of Gl 229 B (Oppenheimer et al., 1995). Below, adaptive optics images obtained with ADONIS/SHARP and the circular variable filter ($\lambda/\Delta\lambda \approx 60$) at three distinct wavelength bands on and off molecular absorption bands are shown. The image scale was 0.035"/pixel. Four two-minute exposures were coadded for each frame. No image deconvolution has been applied.

2. The Luminosity Evolution of Young Brown Dwarfs and Giant Planets

Younger brown dwarfs will have a higher luminosity, their bolometric luminosity L_{BD} evolves with time t as $L_{BD} \propto t^{-1.2}$ (Black, 1980, Burrows et al., 1995¹) Pre-main-sequence stars exhibit a tem-

poral luminosity evolution similar to brown dwarfs. However, their luminosity L_{PMS} decreases much slower than that of brown dwarfs (e.g. $L_{PMS} \propto t^{-0.7}$ for a pre-main-sequence star with a mass of 0.5 M_\odot and an age between 10^5 and 10^8 yr, D'Antona & Mazzitelli, 1994).

Figure 2 illustrates the evolution of the luminosity ratio of a 0.02 M_\odot brown dwarf and a 0.50 M_\odot star. Whereas at an age of 10^6 yr to 10^7 yr the luminosity ratio is in the range of ≈ 0.1 to 0.03, it will be two orders of magnitude smaller at an age of 10^9 yr. It will become increasingly harder to detect a brown dwarf next to an "older" pre-main-sequence star or even a main-sequence star than next to a young pre-main-sequence star – always assuming that the star and the brown dwarf are coeval. Studies of the individual components of pre-main-sequence binaries revealed that most of them are indeed coeval (Hartigan et al., 1994, Brandner & Zinnecker, 1997).

Because of the smaller brightness difference, it should be much easier to de-

¹Note that these calculations did not consider the fact that brown dwarfs with masses $\geq 13 M_{\text{Jupiter}}$ will start Deuterium burning and might be considerably brighter over a short period of time.

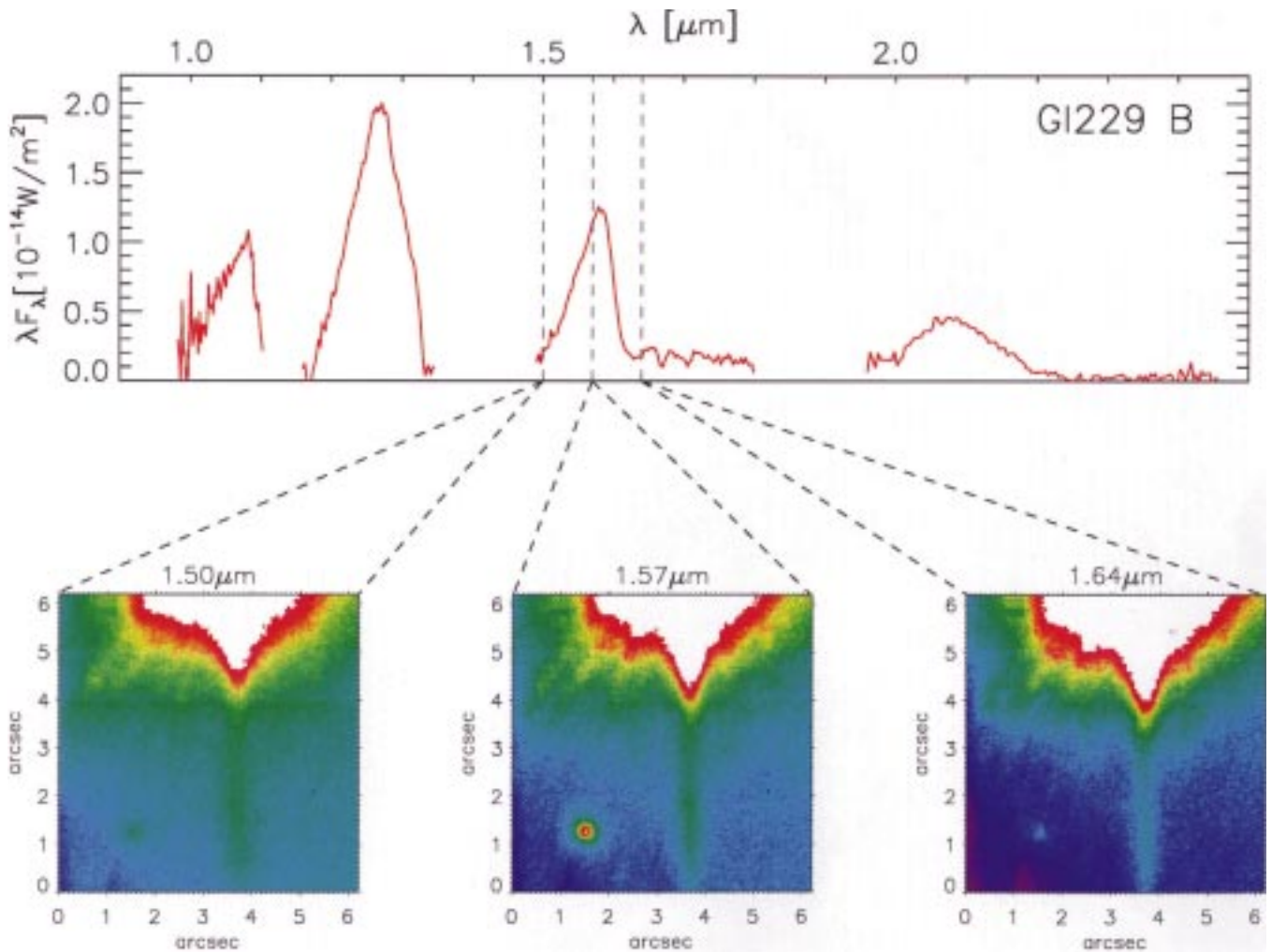


Figure 1: Top: Low-resolution spectrum of GI 229 B (Oppenheimer et al., 1995). Bottom: GI 229 B observed with adaptive optics (ADONIS) at the ESO 3.6-m telescope on March 24, 1997 in wavelength bands centred on molecular absorption bands and in the continuum. At the wavelength of a strong CH_4 absorption band ($1.64 \mu\text{m}$), GI 229 B is about 2 mag fainter than in the nearby “continuum” ($1.57 \mu\text{m}$). North is up and east is to the left.

tect and resolve young brown dwarfs and young giant planets as companions to T Tauri stars than their more evolved (older) counterparts. As explained above, observations in the near-infrared between $1.0 \mu\text{m}$ and $2.5 \mu\text{m}$ are suited best!

3. The Sample

Contrary to classical T Tauri stars, weak-line T Tauri stars no longer possess massive circumstellar disks (e.g. Beckwith et al., 1990). In weak-line T Tauri stars, the circumstellar matter was either accreted onto the central star or redistributed to form planetesimals or – via disk fragmentation – to form directly giant planets or brown dwarfs.

Based on photometric and spectroscopic studies of ROSAT sources (Alcalá et al., 1995, Kunkel et al., in preparation) we have selected an initial sample of 200 weak-line T Tauri stars in the Chamaeleon T association (cf. Fig. 3) and the Scorpius-Centaurus OB association. Proper-motion studies (e.g. Frink et al., 1997) as well as radial-velocity measurements (e.g. Covino et al., 1997) helped to select member stars of

the associations. In the course of follow-up observations visual and spectroscopic binary stars were identified

(Brandner et al., 1996, Covino et al., 1997, Köhler et al., in prep.) and excluded from our final list as the complex

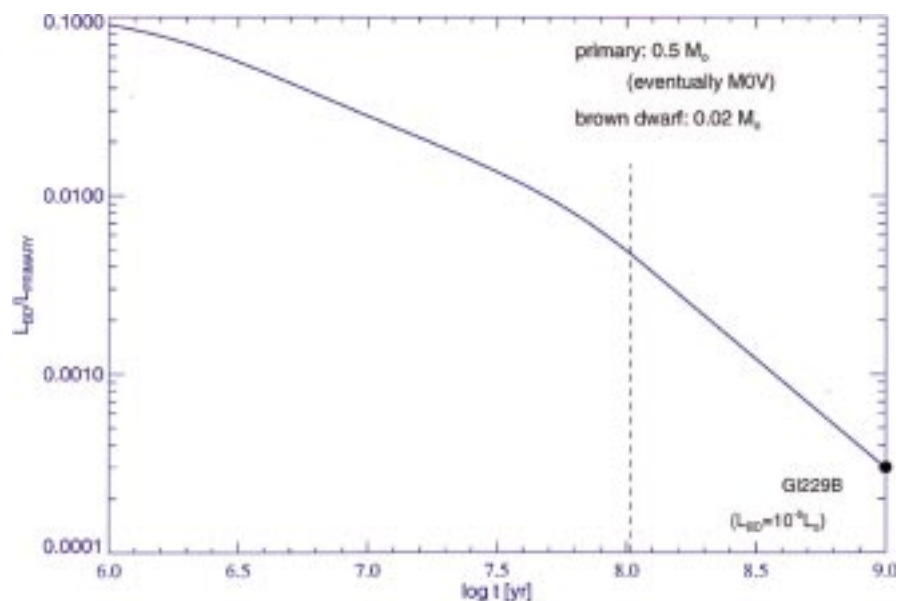


Figure 2: Temporal evolution of the luminosity ratio of a $0.02 M_{\odot}$ brown dwarf and a $0.50 M_{\odot}$ star (“primary”), which after $\approx 10^8 \text{ yr}$ (dashed line) eventually settles on the main sequence as an M0-type star. The current location of GI 229 B is indicated by a black dot.

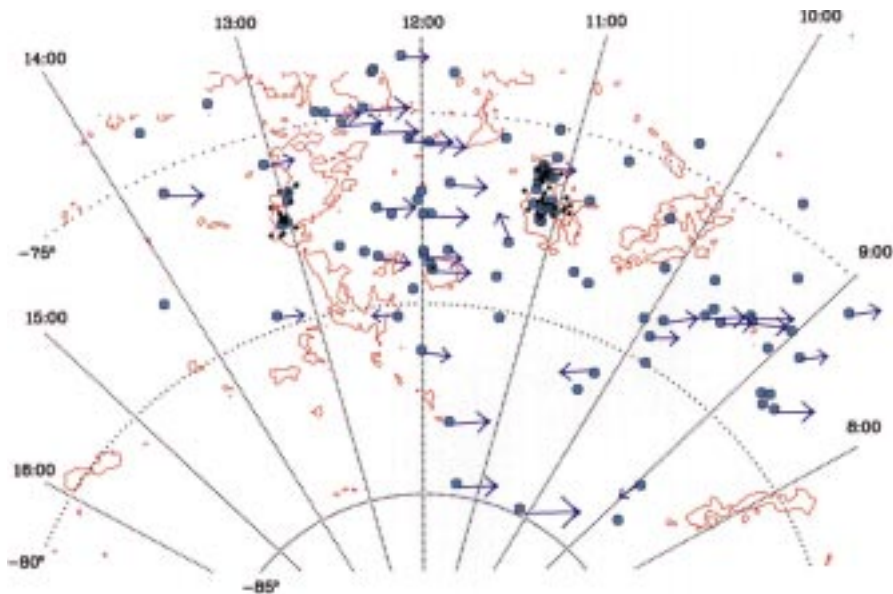


Figure 3: Spatial distribution of classical (black dots) and weak-line (turquoise dots) T Tauri stars in the Chamaeleon T association. Proper motions are indicated by blue arrows. IRAS 100 μm contours indicate the location of the dark clouds.

dynamics and gravitational interactions in binary systems might aggravate or even completely inhibit the formation of planets (depending on physical separation of the binary components and their mass-ratio). We ended up with a final sample of about 70 presumably single weak-line T Tauri stars.

4. Observations with Adaptive Optics and HST

The big questions are:

- What are the time scales for disk dissipation?

- When does planet formation take place?
- How common are young planetary systems?
- What type of environment encourages the formation of planetary systems? (T or OB associations?)

In Period 58 we started a systematic search for substellar companions to single weak-line T Tauri stars using ADONIS/SHARP at the ESO 3.6-m telescope. In total, about 50 G- and K-type weak-line T Tauri stars will be observed. In addition, from July 1997 on, 24 M-type weak-line T Tauri stars will

be surveyed for faint brown dwarf or giant planet companions with HST/NICMOS.

First results of our survey are shown in Figure 4. Follow-up observations are necessary in order to verify that the T Tauri star and its presumed companion form a common proper-motion pair. Adaptive-optics images in and out of molecular bands (cf. Figure 1, see also Rosenthal et al., 1996) will then provide a first estimate of the effective temperature of the companion

Depending on the brightness difference between the primary and the low-mass companion, our survey will be sensitive to separations down to 0.20", i.e. 30 AU (comparable to the semi-major axis of the orbit of Neptune) at a distance of 150 pc.

The new generation of 8-m- to 10-m-class telescopes in combination with adaptive optics will enable us to extend this survey to substellar companions situated even closer to their central star. From 1998 on, the Keck II telescope will be equipped with adaptive optics (diffraction limited at 2 μm) and thus be able to resolve separations as small as 15 AU at a distance of 150 pc. Adaptive optics at the first VLT telescope should become on-line in 2000. Diffraction limited imaging at 1 μm would give a spatial resolution for faint companions of about 8 AU at 150 pc.

Also in 2000, the first segment of the VLTI as well as the Keck interferometer (equipped with adaptive optics) should become operational. Both interferometers will ultimately provide a resolution of 3 mas at 2 μm (less than 1 AU at 150 pc). Thus, also the inner region of young

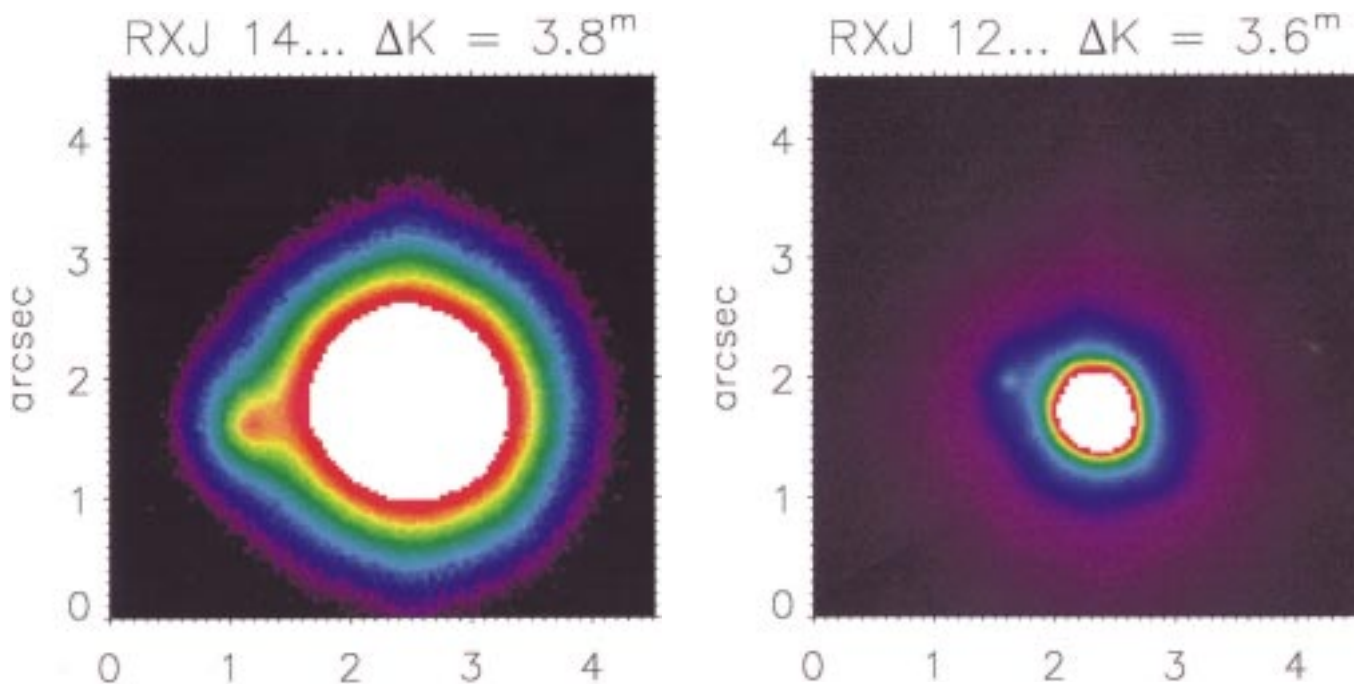


Figure 4: Candidates for substellar companions of two weak-line T Tauri stars in Chamaeleon (ADONIS/ESO 3.6-m, March 1997). Follow-up observations are necessary to discern physical companions from chance projections and to probe the physical properties of the companions. North is up and east is to the left.

planetary systems will finally become resolvable.

Acknowledgements: We would like to thank Drs. Eva K. Grebel and Hans Zinnecker for helpful discussions and comments.

References

Alcalá J.M., Krautter J., Schmitt J.H.M.M. et al. 1995, *A&AS* **114**, 109.
 Allard F., Hauschildt P.H. 1995, *ApJ* **445**, 433.

Beckwith S.V.W., Sargent A.I., Chini R.S., Guesten R. 1990, *AJ* **99**, 924.
 Black D.C. 1980, *ICARUS* **43**, 293.
 Brandner W., Alcalá J.M., Kunkel M., Moneti A., Zinnecker H. 1996, *A&A* **307**, 121.
 Brandner W., Zinnecker H. 1997, *A&A* **321**, 220.
 Burrows A., Hubbard W.B., Lunine J.L. et al. 1995, *Nature* **375**, 299.
 Covino E., Alcalá J.M., Allain S., et al. 1997, *A&A*, in press.
 D'Antona F., Mazzitelli I. 1994, *ApJS*, **90**, 467.
 Frink S., Röser S., Neuhäuser R., Sterzik M.F. 1997, *A&A*, **325**, 613.

Hartigan P., Strom K.M., Strom S.E. 1994, *ApJ* **427**, 961.
 Mayor M., Queloz D. 1995, *Nature*, **378**, 355.
 Marcy G.W., Butler R.P. 1996, *ApJ* **464**, L147.
 Nakajima T., Oppenheimer B.R., Kulkarni S.R. et al. 1995, *Nature* **378**, 463.
 Oppenheimer B.R., Kulkarni S.R., Matthews K., Nakajima T. 1995, *Science* **270**, 1478.
 Rosenthal E.D., Gyrrwell M.A., Ho P.T.P. 1996, *Nature* **384**, 243.

W. Brandner
 brandner@astro.uiuc.edu

The ESO Exhibition at the IAU General Assembly in Kyoto, Japan

Like at previous IAU General Assemblies, ESO maintained an information stand with up-to-date information about the organisation and the current status

of the VLT project. A scale model of the VLT was on display and the stand also featured daily screenings of ESO videos. Located in the Event Hall next to

the e-mail terminals, the 35-square-metre ESO stand quickly evolved into "a meeting place at the meeting", serving as a venue for many informal discussions as well as a contact point for ESO staff and a steady stream of visitors wishing to learn more about ESO's activities.

Other exhibitors included the Gemini Project, the National Astronomical Observatory of Japan (including SUBARU), ROSAT, NRAO, ASP and NASDA (the Space Agency of Japan) as well as commercial exhibitors such as Carl Zeiss, Toshiba, Kluwer Academic Publishers, Cambridge University Press, etc.

C. MADSEN



Figure 1

Figure 1: With the Emperor and the Empress in attendance, IAU President Prof. L. Woltjer opens the General Assembly.

Figure 2: ESO's stand was located between the National Observatory of Japan and NASDA, in the huge "Event Hall".

Figure 3: The ESO information stand – "a meeting place at the meeting".



Figure 2



Figure 3